An invited *Perspective* for Nature Geoscience

Increased frequency of extreme El Niño associated with a 1.5 °C warming

Guojian Wang[1,2], Wenju Cai*[,1,2], Lixin Wu[1], Agus Santoso[3], Mike McPhaden[4], & Xiaopei Lin[1]

1. Physical Oceanography Laboratory/CIMSST, Ocean University of China and Qingdao National Laboratory for Marine Science and Technology, Yushan Road, Qingdao 266003, China
2. CSIRO Oceans and Atmosphere, Aspendale, Victoria, Australia
3. Australian Research Council (ARC) Centre of Excellence for Climate System Science, Level 4 Mathews Building, The University of New South Wales, Sydney 2052, Australia
4. NOAA/Pacific Marine Environmental Laboratory, Seattle, Washington, USA

*<u>*Corresponding author: Wenju Cai*</u>: wenju.cai@csiro.au
Guojian Wang: guojian.wang@csiro.au
Lixin Wu: lxwu@ouc.edu.cn
Agus Santoso: a.santoso@unsw.edu.au
Michael J. McPhaden: michael.j.mcphaden@noaa.gov
Xiaopei Lin: linxiaop@ouc.edu.cn

The December 2015 global climate change conference in Paris adopted an international accord aimed at transforming the world's fossil fuel-driven economy within decades and slowing the pace of global warming to below 2 °C relative to preindustrial levels, with an aspirational target of 1.5 °C. Little is known about the impact of a 1.5 °C-warming on climate extremes, such as the frequency of extreme El Niño events. Such extremes severely affect weathers, agriculture, ecosystems, public health and economies worldwide, and should be a factor in the consideration of targets to avoid dangerous climate change. By estimating changes induced by a 1.5 °C-warming, here we argue that the risk of an increased frequency of extreme El Niño events is still high, although lower than that at 2 °C-warming. Moreover, the risk may even intensify for a century after the global mean temperature has stabilised. An increased risk associated with extreme La Niña under a projected business-as-usual emission scenario, however, can be avoided.

For a given rise in global mean temperature (GMT), regional climate impacts and local capacities to adapt vary vastly from one region to another. As such, debates are moot as to what level of climate change can be considered ‘dangerous’ and what level of global warming must be avoided[1,2]. The local impacts projected for a 2 °C warming are beyond what many societies, particularly small island states, would be able to cope with, particularly in terms of risk of extreme events such as tropical cyclones, droughts and floods, and as well extreme heat waves[3,4,5,6]. A lower warming level has been called for and the historic Paris agreement responded with an aspirational target of 1.5 °C.

However, only a limited number of studies have considered emission scenarios that are consistent with a 1.5 °C limit[7,8,9,10,11,12,13], and even fewer on expected impacts. The limited number of studies, carried out mainly for comparison with a 2 °C warming, showed that the projected frequency of heat extremes at 1.5 °C-warming would be reduced by 50% from that associated with 2 °C warming[14]. Further, limiting warming to 1.5 °C would reduce the rate of not only sea level rise, but also the melting of the polar ice sheets, which contributes directly to the risk of large-scale sea level rise[15,16,17]. The full spectrum of the impact from a sustained 1.5 °C warming is still far from clear, including the impact on climate extremes. We argue that understanding the impact on the frequency of extreme El Niño events should be part of the assessment of what constitutes dangerous climate change because of its far reaching global impacts[18].

During the 1997 extreme El Niño (see Box 1 for a definition), the western Pacific convection zone moved to the eastern equatorial Pacific and the Intertropical Convergence Zone (ITCZ) shifted southwards towards the equator. This massive reorganisation of the atmospheric circulation induced severe impacts worldwide. Droughts plagued regions surrounding the western Pacific[19,20]. Catastrophic floods occurred in parts of Ecuador and northern Peru[18,19,27] while neighbouring regions to the south and north experienced severe droughts. The South Pacific Convergence Zone (SPCZ), the largest rainband in the Southern Hemisphere, shifted toward the equator by up to 1000 km[28,29], spurring floods and droughts in south Pacific countries and shifting extreme cyclones to regions normally not affected by such events. The anomalous conditions caused widespread environmental disruption, including the disappearance of marine life and consequent decimation of the native bird populations in the Galapagos Islands[30,31], and severe bleaching of corals in the Pacific and beyond[32,33].

The 1997 event was followed by an extreme La Niña in 1998 (see Box 1 for a definition), the strongest of the 20th century, with generally opposite climatic impacts to those seen in 1997.

These impacts included flooding in the West Pacific[34,35], and increased land-falling West Pacific cyclones and Atlantic hurricanes, killing tens of thousands of people[34,35,36,37]. The 1997 extreme El Niño and 1998 extreme La Niña together claimed over 50,000 lives, dislocated over 250 million people, and caused tens of billions in damage around the world[34,35,36,37,38,39].

Recent studies have shown that under the Representative Concentration Pathway 8.5 (RCP8.5)[40,41], greenhouse warming leads to an increased frequency of extreme El Niño and extreme La Niña[21,24,42]. Under the RCP8.5 scenario, the multi-model ensemble average of global mean temperature increases by about 4.5 ^{o}C by 2100. Here we estimate changes in the frequency of these extremes at the 1.5 ^{o}C-warming level and show that, despite a reduction from the 2 ^{o}C warming level, the frequency of extreme El Niño still doubles from that of the preindustrial level. Further, we find the maximum risk emerges long after the targeted GMT limit is reached. On the other hand, the frequency of extreme La Niña does not increase under 1.5 or 2 ^{o}C warming.

Increased frequency of extreme El Niño at the 1.5 ^{o}C warming

In the Climate Model Intercomparison Project's Phase 5 (CMIP5)[43], the RCP2.6 (or RCP3PD) emission scenario is a "peak-and-decline" pathway that leads to low greenhouse gas concentration levels[40,41] and produces a peak GMT rise close to 1.5 ^{o}C above the preindustrial level. A total of 13 models under this emission scenario are able to generate extreme El Niño and La Niña events[21,24] and produce a 1.5 ^{o}C global mean temperature (GMT) rise from the preindustrial level. To assess the frequency changes, we first calculate 31-year running averages to determine when 1.5 ^{o}C GMT limit is achieved in each model. We then compare the number of extreme El Niño events from the 31-year period centred at the 1.5 ^{o}C warming aggregated across the 13 models with that from the model aggregates of the last 31 years of the preindustrial period (1869-1899). We focus on the season of December, January, and February, in which an El Niño event peaks. As such, we have a large sample of 403 years (13 models x 31 years) for each of the warming and preindustrial cases to determine the frequency change.

Because the warming in the majority of these experiments under RCP2.6 do not reach 2 ^{o}C, we adopted the approach[44] in utilising RCP2.6 for a 1.5 ^{o}C warming and RCP4.5 for a 2 ^{o}C warming to explore their differences. The RCP4.5 pathway is a scenario in which the total radiative forcing is stabilized shortly after 2100, without overshooting the long-run radiative forcing target[40,41]. The frequency of extreme El Niño for the 2 ^{o}C-warming climate is similarly estimated using 31-year outputs centred at the year when 2 ^{o}C warming is reached.

The frequency of extreme El Niño increases from 4.5 events per 100 years (or one event per 22 years) in the preindustrial period (Fig. 1a) to 10.4 events per 100 years (or about one event per 10 years) at a 1.5 ^{o}C warming, i.e., a 130% increase. The inter-model consensus is strong, with none of the models producing a reduction. The increase is statistically significant above the 99% confidence level (i.e., greater than three times of the standard deviation of internal variability of the preindustrial period; see Methods). The frequency at 1.5 ^{o}C warming is 65% greater than the frequency during the 20th century, with 6.3 events per 100 years (or about one event per 16 years) averaged across the 13 models over the 1900-1999 period.

The frequency at the 2 ^{o}C warming is 12.9 events per 100 years, or one event per 8 years. This is 24% higher than for 1.5 ^{o}C warming (Fig. 1b), approximately what is expected from the linear assumption in terms of change per ^{o}C of global warming, which would yield a 25% difference. The inter-model consensus is high, with only two models generating a lower frequency at 2 ^{o}C than at 1.5 ^{o}C warming. The central point is that despite the reduction of extreme El Niños from 2 ^{o}C to 1.5 ^{o}C warming, the frequency of extremes at 1.5 ^{o}C warming is still high compared to preindustrial.

Consistent with findings from previous studies[21], there is no statistically significant difference in the intensity of extreme El Niño between either of the two warming levels and the preindustrial level. Composite of rainfall total for extreme El Niño events shows that the spatial pattern and the associated rainfall teleconnection remain overall similar in the two periods (Fig. 1c, d, and stars of Fig. 1a, b), suggesting that, at a given location, extreme El Niño impacts will repeat more frequently in the warming climate.

Robust underpinning process

Mean state circulation changes underpin the increased frequency of extreme El Niño. Migration of the ITCZ to the equator in the eastern Pacific (see Box 1), which characterises an extreme El Niño, is supported by a reduced "off equatorial-minus-equatorial" (area of red solid rectangle minus red dashed rectangle, Fig, 2a, b) surface temperature gradient[21] (see

Box 1). Under RCP8.5, this meridional gradient decreases with a projected warming faster in the equatorial Pacific than off-equatorial regions, and faster in the eastern equatorial Pacific warming than the surrounding regions[45]. As a consequence, it is easier to induce extreme El Niño even if temperature variability does not change[21]. There is still a strong and robust reduction in the meridional temperature gradient with a 1.5 ^{o}C and 2 ^{o}C warming (Fig. 2a, b), underscored by the strong inter-model consensus (red bars in Fig. 2c, d). The reduction is seen in every model for the 1.5 ^{o}C warming, and only one model produces a weak increase for the 2 ^{o}C warming.

A direct consequence of the 1.5 ^{o}C or 2 ^{o}C warming target is no statistically significant increase of extreme La Niña, in contrast to that projected under RCP8.5[24]. Extreme La Niña events feature concentrated atmospheric convection in the Maritime region but reduced convection in the central equatorial Pacific. Hence, ocean-atmosphere anomalies involved in the associated positive feedbacks are influenced by an enhanced Maritime-minus-central Pacific temperature gradient (Box 1, area of blue rectangle minus blue dashed box, Fig. 2a, b). Under RCP8.5, the Maritime continent warms substantially faster after 2050 than the central equatorial Pacific after 2050 (Figure not shown), underpinning the increase in the frequency of extreme La Niña events[24]. Under RCP2.6 or RCP4.5, there is no intermodel consensus in the change of the zonal temperature gradient, with about half of the models generating an increase and the other half generating a reduction (blue bar in Fig. 2c, d). Under RCP2.6 and RCP4.5, because a large portion of the Maritime region is ocean area, a substantial warming contrast between the Maritime region and the central Pacific is not yet established at these warming levels. Consequently, there is no inter-model consensus in the frequency of extreme La Niña from the preindustrial level and hence no definitive change. This result means that the catastrophic combination of an extreme El Niño followed by an extreme La Niña, as seen in the 1997 and 1998 may not occur as often in these two scenarios as in the business-as-usual projection of the RCP8.5[24].

Temporal evolution and risk after a warming stabilises

The risk of an increased frequency of extreme El Niño appears to intensify linearly with the rise in GMT. For instance, the increase at the 1.5 ^{o}C warming in RCP2.6 is approximately 75% of that at a 2 ^{o}C warming in RCP4.5 (Fig. 1b). To reveal whether this linearity is systematic and robust, we examine the evolution of the GMT change, the meridional temperature gradient change, and the frequency of the extreme El Niño using 31-year sliding periods in each of 13 models forced under the historical emission and the RCP2.6 scenario, and in terms of multi-model ensemble average (Fig. 3a, b, note the reversed gradient sign). The multi-model ensemble average gradient (Fig. 3a) and frequency (Fig. 3b) at 1.5 ^{o}C warming (**light green filled region**) are 0.3 ^{o}C (red filled circle, Fig. 3a) and 10.3 events per 100 year (purple filled circle, Fig. 3b), respectively. The frequency is comparable to that aggregated from outputs when each individual model is at a 1.5 ^{o}C warming. Although the ensemble GMT rise does not quite reach 2 ^{o}C, the evolution shows that during the transient increase of CO_2 toward 2 ^{o}C warming, the weakening meridional gradient and the increasing frequency change roughly linearly with the GMT rise. Thus, the approximately 25% difference between the 1.5 ^{o}C and 2 ^{o}C warming is underpinned by this linearity. This is further confirmed by changes in the last 31-year period, when the multi-model ensemble GMT rise is close to 2 ^{o}C (**light orange filled region**), showing an averaged frequency of 13 events per 100 years (purple star, Fig. 3b), similar to that shown in Fig. 1b (purple star).

More importantly though, the risk of increased frequency continues to grow after the GMT peaks and stabilises, supported by a further weakening in the meridional temperature gradient (Fig. 3a). The time scale for which further weakening may last, and the eventual frequency to which the further weakening may lead, are of great interest. There are only five models out of the 13 that have outputs beyond 2100, but we can use these to provide a gauge, without forgetting that an ensemble of 5 models will contain significant interdecadal variability. The weakening meridional gradient, established during the transient increase of CO_2, does not just persist but actually intensifies for about a century before reversing its trend to be in line with the GMT (Fig. 3c). The frequency of extreme El Niños, though defined using a discrete threshold value of rainfall and hence more fluctuating, essentially follows the same evolution, featuring a further increase after the GMT stabilises. This behaviour is somewhat similar to the response of sea level[46,47,48], but what is surprising is that even the temperature gradient, which measures the difference between two locations, responds in this manner.

Although the continuous weakening of the gradient and increase in the frequency (Fig. 3c, d) commence from a warming level close to 2 ^{o}C, there is no reason to believe that a commencement from a 1.5 ^{o}C would generate a completely different evolution, given that pathways to a 1.5 ^{o}C and 2 ^{o}C warming are similar[13,44]. It is not clear whether the gradient and the frequency would ever recover to the preindustrial level. It seems that if the recovery were to occur, it would take many centuries to do so (Fig. 3c, d). The central point is that the risk assessed using outputs from the transient increase of CO_2 may be substantially under-estimated.

Toward a full impact assessment of a 1.5 °C warming

We have shown that the frequency of extreme El Niño at a 1.5 °C warming, though lower than at 2 °C, doubles that of the preindustrial level. During the transient increase of CO_2, the frequency of extreme El Niño and the underpinning meridional surface temperature gradient in the eastern equatorial Pacific evolve linearly with the GMT and CO_2. This implies that any increase in CO_2 directly leads to a higher risk of an increased frequency of extreme El Niño events. However, even after the warming stabilises, the frequency still continues to increase and the meridional gradient continues to weaken for a century. It is unclear whether this long persistence depends on a stabilized warming level, but is suggestive of a positive feedback process that operates between the meridional gradient and the atmospheric circulation involving El Niño. If this feedback does operate, then what the process might be that eventually leads to its demise, and what frequency of extreme El Niño will be in the stabilised 1.5 °C warming world, are some important questions to address. Properly resolving these issues will require a large ensemble of multi-century long experiments than currently available, but is an integrated part of assessing the full impact of the 1.5 °C warming, which at present is far from complete. The 1.5 °C aspirational target provides a mandate to explore the 1.5 °C-warming world, but whether it is a target that avoids dangerous climate change is yet to be fully assessed.

Methods

We used CMIP5 model outputs of surface temperature and precipitation for the boreal winter season (December, January, and February), in which an El Niño event matures. We took a 31-year period centered at a warming of 1.5 °C under the RCP2.6 scenario, and 2 °C under RCP4.5, relative to the preindustrial period of 1869–1899. Note that those simulations are transient. Equilibrium state does not exist for most models. One initial condition member from each model is used with equal weight. Results in Fig. 1 are aggregated over all 13 selected models, able to produce extreme El Niño and La Niña (see Box 1 for definition) and a warming of 1.5 °C from the 1869–1899 level. We use a bootstrap method to examine whether the difference in frequency of extreme events at a 1.5 °C and in the preindustrial period is statistically significant. There is a total of 403 years. These are re-sampled randomly to construct another 10,000 realisations of 403 records. In the random re-sampling process, any extreme event is allowed to be selected again. For instance, the standard deviation of the extreme El Niño frequency in the inter-realization is 1.2 event per 100 years, far smaller than the difference between two periods, indicating a strong statistical significance.

References

1. Schellnhuber, H. J., Cramer, W., Nakicenovic, N., Wigley, T. M. L. & Yohe, G. (eds) *Avoiding Dangerous Climate Change* (Cambridge Univ. Press, 2006).
2. Mahlstein, I., Knutti, R., Solomon, S. & Portmann, R. W. Early onset of significant local warming in low latitude countries. *Environ. Res. Lett.* **6**, 034009 (2011).
3. *Earth Negotiations Bulletin* (IISD Reporting Services, 2008).
4. *Submissions from Parties* FCCC/KP/AWG/2009/MISC.1/Add.1 (UNFCCC, 2009).
5. Meinshausen, M., *et al*. Greenhouse-gas emission targets for limiting global warming to 2 ^{o}C. *Nature* **458**, 1158-1162 (2009).
6. *Climate Change 2014: Impacts, Adaptation, and Vulnerability* (eds Field, C. B. *et al.*) 1–32 (IPCC, Cambridge Univ. Press, 2014).
7. Moss, R., *et al.* The next generation of scenarios for climate change research and assessment. *Nature* **463**, 747–756 (2010).
8. Ranger, N. *et al.* Is it possible to limit global warming to no more than 1.5 °C? *Climatic Change* **111**, 973–981 (2012).
9. Luderer, G. *et al.* Economic mitigation challenges: How further delay closes the door for achieving climate targets. *Environ. Res. Lett.* **8**, 034033 (2013).
10. Azar, C., Johansson, D. J. A. & Mattsson, N. Meeting global temperature targets—the role of bioenergy with carbon capture and storage. *Environ. Res. Lett.* **8**, 034004 (2013).
11. Rogelj, J., McCollum, D. L., Reisinger, A., Meinshausen, M. & Riahi, K. Probabilistic cost estimates for climate change mitigation. *Nature* **493**, 79–83 (2013).
12. Rogelj, J., McCollum, D. L., O'Neill, B. C. & Riahi, K. 2020 emissions levels required to limit warming to below 2 °C. *Nature Clim. Change* **3**, 405–412 (2013).
13. Rogelj, J., *et al.* System transformations for limiting end-of-century warming to below 1.5°c. *Nature Clim. Change* **5**, 519-527 (2015).
14. Fischer, E. M. & Knutti, R. Anthropogenic contribution to global occurrence of heavy-precipitation and high-temperature extremes. *Nature Clim. Change* **5**, 560-564 (2015).

15. Schaeffer, M., Hare, W., Rahmstorf, S. & Vermeer, M. Long-term sea-level rise implied by 1.5 °C and 2 °C warming levels. *Nature Clim. Change* **2**, 867–870 (2012).
16. Levermann, A., *et al*. The multimillennial sea level commitment of global warming. *Proc. Natl. Acad. Sci. U. S. A.* **110**, 13745–13750 (2013).
17. Dutton, A., *et al*. Sea level rise due to polar ice-sheet mass loss during past warm periods. *Science* **349**, DOI: 10.1126/science.aaa4019 (2015).
18. McPhaden, M. J., Zebiak, S. E. & Glantz, M. H. ENSO as an integrating concept in Earth science. *Science* **314**, 1740-1745 (2006).
19. Philander, S. G. H. Anomalous El Niño of 1982-83. *Nature* **305**, 16 (1983).
20. McPhaden, M. J. El Niño: The child prodigy of 1997-98. *Nature* **398**, 559-562. doi:10.1038/19193 (1999).
21. Cai, W. *et al*. Increasing frequency of extreme El Niño events due to greenhouse warming. *Nature Clim*. *Change* **4**, 111–116 (2014).
22. Lengaigne, M., & Vecchi, G. A. Contrasting the termination of moderate and extreme El Niño events in coupled general circulation models. *Clim. Dyn* **35**, 299-313(2009).
23. Chiodi, A. M., & Harrison, D. E. Characterizing warm-ENSO variability in the equatorial Pacific: An OLR perspective. *J. Clim.* **23**, 2428–2439 (2010).
24. Cai, W. *et al*. More frequent extreme La Niña events under greenhouse warming. *Nature Clim. Change* **5**, 132-137 (2015).
25. Takahashi, K., Montecinos, A., Goubanova, K., and Dewitte, B. ENSO regimes: Reinterpreting the canonical and Modoki El Niño. *Geophys. Res. Lett.* **38**, L10704, doi:10.1029/2011GL047364 (2011).
26. Dommenget, D., Bayr, T., & Frauen, C. Analysis of the non-linearity in the pattern and time evolution of El Niño southern oscillation. *Clim. Dyn.* **40**, 2825–2847. DOI 10.1007/s00382-012-1475-0 (2013).
27. Vos, R., Velasco, M., & Edgar de Labastida, R. Economic and social effects of El Niño in Ecuador, 1997–1998. Inter-American Development Bank Sustainable Development Dept. Technical papers series POV-107, 38pp (1999).
28. Vincent, E. M. *et al.* Interannual variability of the South Pacific Convergence Zone and implications for tropical cyclone genesis. *Clim. Dyn.* **36**, 1881–1896 (2011).
29. Cai, W. *et al.* More extreme swings of the South Pacific convergence zone due to greenhouse warming. *Nature* **488**, 365–369 (2012).
30. Merlen, G., The 1982–1983 El Niño: Some of its consequences for Galapagos wildlife, *Oryx* **18**, 210–214 (1984).

31. Valle C. A. *et al.* The Impact of the 1982–1983 E1 Niño-Southern Oscillation on Seabirds in the Galapagos Islands, Ecuador. *J. Geophys. Res*. **92**, 14,437–14,444 (1987).
32. Glynn, P. W., & de Weerdt, W. H. Elimination of two reef-building hydrocorals following the 1982–83 El Niño. *Science* **253**, 69–71 (1991).
33. Aronson, R. B., *et al.* Coral bleach-out in Belize, *Nature* **405**, 36 (2000).
34. Kunii, O., Nakamura, S., Abdur, R., and Wakai, S. The impact on health and risk factors of the diarrhoea epidemics in the 1998 Bangladesh floods. *Public Health* **116**, 68–74 (2002).
35. Jonkman, S. N. Global Perspectives on Loss of human life caused by floods. *Natural Hazards* **34**, 151-175 (2005).
36. Bell, G.D. *et al.* Climate Assessment for 1998. *Bull. Amer. Meteor. Soc*. **80**, 1040–1040 (1999).
37. Kerle, N., Froger, J. L., and Oppenheimer, C., and Van Wyk De Vries, B. Remote sensing of the 1998 mudflow at Casita volcano, Nicaragua. *International Journal of Remote Sensing* **24**, 4791-4816 (2003)
38. Sponberg, K. Compendium of Climatological Impacts, University Corporation for Atmospheric Research Vol. 1 (National Oceanic and Atmospheric Administration, Office of Global Programs, 1999).
39. Del Ninno, C. & Dorosh, P. A. Averting a food crisis: Private imports and public targeted distribution in Bangladesh after the 1998 flood. *Agric. Econ.* **25**, 337-346 (2001).
40. Moss, R. H. *et al*. The next generation of scenarios for climate change research and assessment. *Nature* **463**, 747-756 (2010).
41. van Vuuren, D.P. *et al*. The representative concentration pathways: an overview. *Climatic Change* **109**, 5-31(2011).
42. Cai, W., *et al*. ENSO under greenhouse warming. *Nature Clim. Change* **5**, 849-859 (2015).
43. Taylor, K. E., Stouffer, R. J. & Meehl, G. A. An overview of CMIP5 and the experimental design. *Bull. Amer. Met. Soc*. **93**, 485–498 (2012).
44. Knutti, R., Rogelj, J., Sedlacek, J., & Fischer, E. M. A scientific critique of the two-degree climate change target. *Nature Geoscience* **9**, 13-18 (2016).
45. Xie, S. P., *et al*. Global warming pattern formation: Sea surface temperature and rainfall. *J. Clim.* **23**, 966–986 (2010).

46. Stouffer, R. J. & Manabe, S. Response of a Coupled Ocean–Atmosphere Model to Increasing Atmospheric Carbon Dioxide: Sensitivity to the Rate of Increase. *J. Climate* **12**, 2224–2237 (1999).

47. Meehl, G. A., *et al*. How much more global warming and sea level rise. *Science* **307** (5716), 1769-1772 (2005).

48. Schaeffer, M., Hare, W., Rahmstorf, S. & Vermeer, M. Long-term sea-level rise implied by 1.5 °C and 2 °C warming levels. *Nature Clim. Change* **2**, 867–870 (2012).

Additional information

Reprints and permissions information is available at www.nature.com/nature. Correspondence and requests for materials should be addressed to WC.

Acknowledgements

W. C. and G. W. are supported by the Australian Climate Change Science Program and a CSIRO Office of Chief Executive Science Leader award. A.S. is supported by the Australian Research Council. PMEL contribution 4427.

Author Contributions

W.C. & G.W. conceived the study, G. W performed all model analysis. W.C. & G.W. write the initial manuscript. All authors contributed to interpreting results, discussion of the associated dynamics, and improvement of this paper.

Author Information Reprints and permissions information are available at: www.nature.com/reprints. The authors declare no competing financial interests. Correspondence and requests for materials should be addressed to Wenju Cai Wenju.Cai@csiro.au

Figure Captions & Box

Figure 1 | Changes in frequency of extreme El Niño events from the preindustrial condition and the associated rainfall pattern. **a**, **b**, Boreal winter relationship between total rainfall (mm per day) in eastern equatorial Pacific (Niño3 area: 5°S-5°N, 150°W-90°W) (**black** box in **c** and **d**) and meridional surface temperature gradient (°C) for the preindustrial condition and the targeted warming levels, respectively. The meridional temperature gradient is defined as the average surface temperature over the off-equatorial region (5°N-10°N, 150°W-90°W) minus the average over the equatorial region (2.5°S-2.5°N, 150°W-90°W) (red solid minus red dashed in **c** and **d**). The **red** and **black** **dots** indicate extreme El Niño (defined as events for which austral summer rainfall in Niño3 area is greater than 5 mm per day[21] and **non-extreme El Niño** events, respectively, for the preindustrial condition and the 1.5 °C. In **b**, **purple** and **grey** dots are for the 2 °C warming condition. A multi-model mean value for those extreme events is also indicated, by a star in each panel. **c**, **d**, Composites of total rainfall (mm per day) during extreme El Niño events, for the preindustrial condition and the 1.5 °C warming world, respectively. The green contour indicates the 5 mm per day isopleth of the total rainfall. Stippling in **d** indicates regions where its differences from **c** are statistically significant above the 95% level, determined by a two-sided Student's *t*-test. The rainfall composites for the 2 °C warming world (not shown here) display a similar pattern to **d**.

Figure 2 | Multi-model ensemble average of surface temperature change from the preindustrial condition. **a**, **b**, Ensemble average surface temperature anomalies for the 1.5 °C warming world and 2.0 °C warming world, respectively. **c**, **d**, Changes in mean zonal (**blue bars**) and meridional (**red bars**) temperature gradient under the 1.5 °C and 2.0 °C warming, respectively, multi-model average and each of the 13 models. The zonal temperature gradient is defined as the average surface temperature over the Maritime region (5°S-5°N, 100°E-125°E) minus the average over the central Pacific region (5°S-5°N, 160°E-150°W)[24] (**Solid blue** minus **dashed blue box,** in **a** and **b**). The meridional temperature gradient is defined as the average surface temperature over the off-equatorial region (5°N-10°N, 150°W-90°W) minus the average over the equatorial region (2.5°S-2.5°N, 150°W-90°W), **solid red** minus **dashed red box** in **a** and **b**.

Figure 3 | Evolution of frequency of extreme El Niño, the associated meridional gradient, and global mean temperature. **a**, Evolution of multi-model ensemble average global mean temperature anomalies (**black curve**) and meridional temperature gradient anomalies (red curve), using 13 available models under the historical emission and RCP2.6 emission scenario (1900-2099). The anomalies are referenced to the preindustrial condition and then averaged in 31-year sliding windows. The sign of meridional temperature gradient is reversed for easy of comparison with the global mean temperature. The two values near the filled circle and star in red indicate the averaged meridional temperature gradient over the 31 years centred at the 1.5 °C warming (light green) and the last 31 years after the global mean temperature stabilises (light orange). The red line and **black line** denote the linear trend for the meridional gradient and global mean temperature, respectively, after the global mean temperature stabilises. **b**, the same as **a**, but for the frequency of extreme El Niño events (purple, events per 100 years). **c** and **d**, The same as **a** and **b**, respectively, but using 5 available models, which extend the simulation to the 23rd century under the RCP2.6 emission scenario. The light pink filled region indicates the period when the global mean temperature decreases but the meridional temperature gradient continues to weaken and the frequency of extreme El Niño continues to increase.

Box 1 | Definition of extreme El Niño, extreme La Niña and the associated dynamic indices

Extreme El Niño. Extreme El Niño events were characterized by an exceptional warming extending into the eastern equatorial Pacific[19,20]. The high sea surface temperatures (SST) leads to an equatorward shift of the Intertropical Convergence Zone (ITCZ), and hence intense rainfall in the equatorial eastern Pacific where cold and dry conditions normally prevail. Niño3 rainfall is thus a good indicator of extreme El Niño[21,22,23] for large-scale atmospheric circulation anomalies. An extreme El Niño is defined as an event during which such massive reorganisation of atmospheric convection takes place, leading to Niño3 rainfall that exceeds 5 mm per day averaged over the El Niño mature season of December, January and February[21]. This definition distinctly identifies the 1982/83 and 1997/98 events as an extreme El Niño.

Eastern equatorial Pacific meridional SST gradients. During extreme El Niño, warming in the eastern equatorial Pacific dramatically weakens the meridional SST gradient. This gradient measures the difference between the northern off-equatorial (8°N, the ITCZ position) and the equatorial Pacific. Convection follows the highest SSTs, as such the ITCZ shifts equatorward[21,22] leading to atmospheric convection and extraordinary rainfall (>5 mm per day) in the normally dry eastern equatorial Pacific. The smaller the gradient, the greater ease for this to occur.

Extreme La Niña. An extreme Niña is not a mirror opposite image of an extreme El Niño[24,25,26]. During extreme La Niña events, coldest sea surface conditions develop in the central Pacific[24,25,26] inhibiting formation of rain-producing clouds there, but enhancing atmospheric convection and rainfall in the western equatorial Pacific. An extreme La Niña is defined as one for which the amplitude of central equatorial Pacific SST (Niño4, (5°S-5°N, 160°E-150°W) is greater than a 1.75-standard deviation (s.d.) value in the La Niña mature season December January and February, and this definition captures the extreme La Niña events of 1988/89 and 1998/99.

Maritime-minus-central Pacific SST gradient. During extreme La Niña events, coldest sea surface conditions develop in the central Pacific, creating an enhanced temperature gradient from the Maritime continent to the central Pacific. This cooling generated stronger easterly winds, which piled up warm water in the western Pacific, increasing the Maritime-central Pacific temperature gradient[24]. This in turn generates further anomalous upwelling of cool water to the surface, and westward surface currents in the Niño4 region, conducive to growth of cold anomalies in the region, in a positive feedback. An increasing trend of this gradient is conducive to occurrences of this positive feedback.

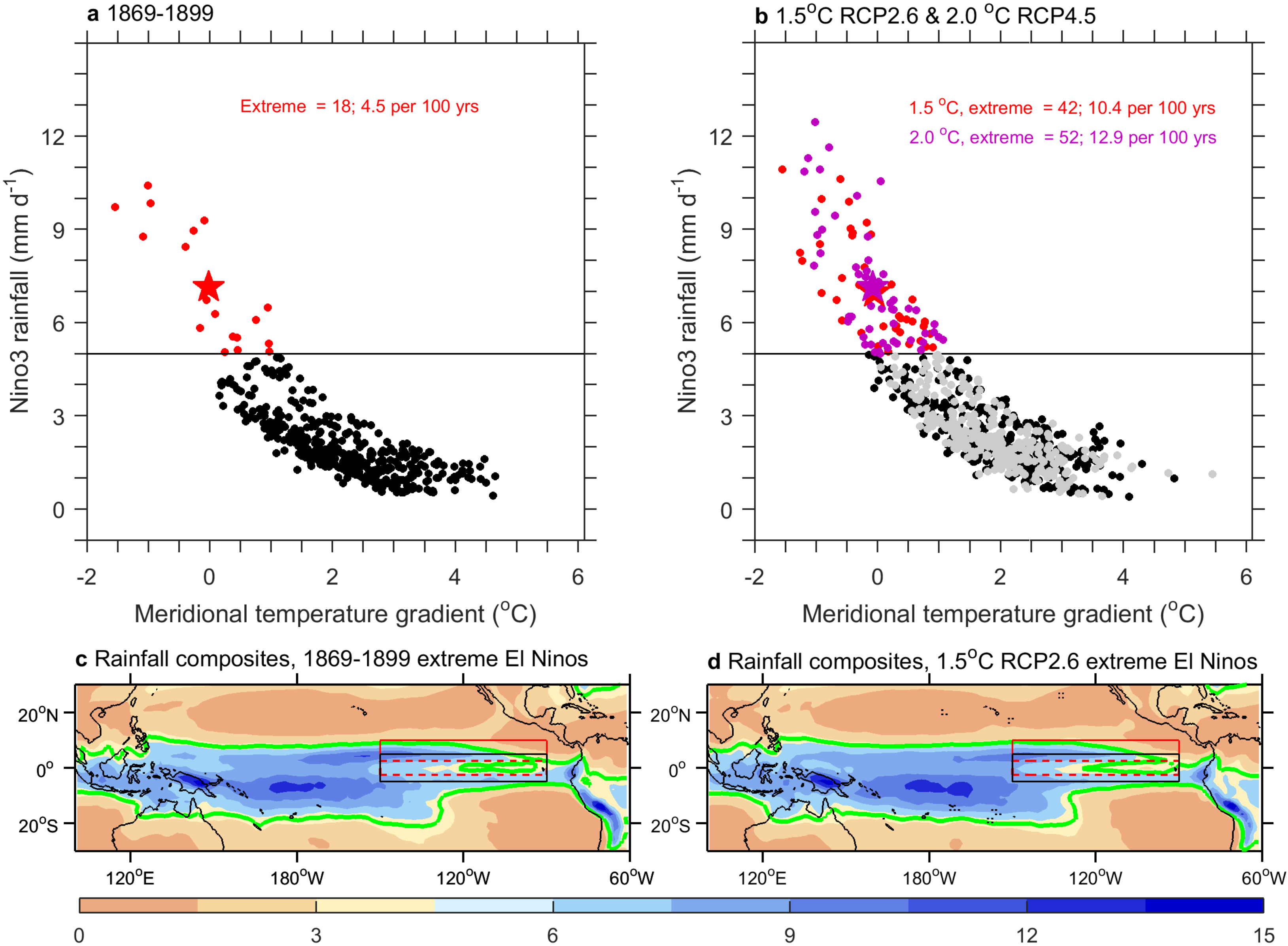

a 1869-1899
Extreme = 18; 4.5 per 100 yrs
Nino3 rainfall (mm d-1)
Meridional temperature gradient (oC)
b 1.5oC RCP2.6 & 2.0 oC RCP4.5
1.5 oC, extreme = 42; 10.4 per 100 yrs
2.0 oC, extreme = 52; 12.9 per 100 yrs
Nino3 rainfall (mm d-1)
Meridional temperature gradient (oC)
c Rainfall composites, 1869-1899 extreme El Ninos
d Rainfall composites, 1.5oC RCP2.6 extreme El Ninos
20oN
0o
20oS
120oE
180oW
120oW
60oW
0
3
6
9
12
15

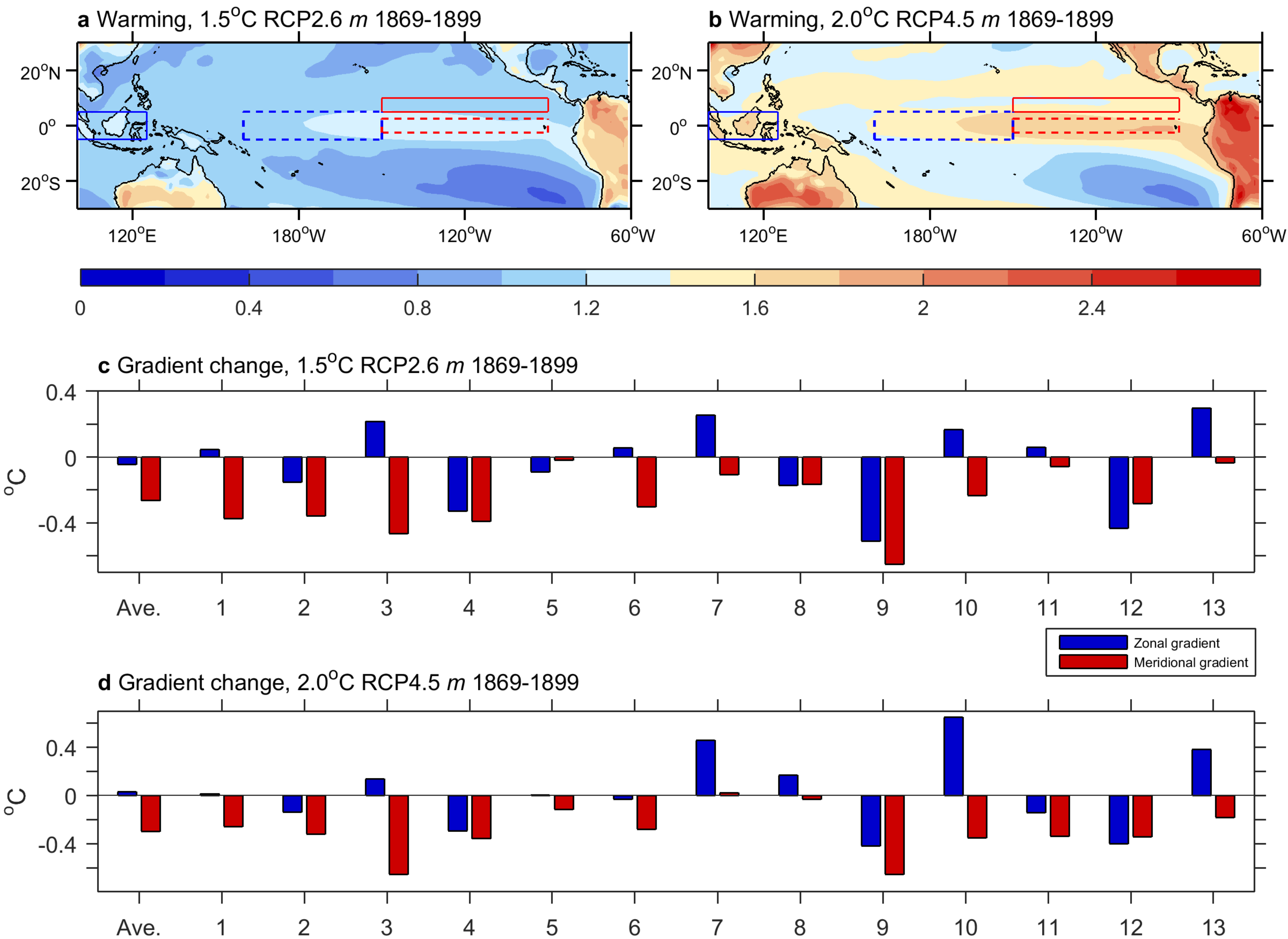

a Warming, 1.5°C RCP2.6 m 1869-1899
b Warming, 2.0°C RCP4.5 m 1869-1899
20°N
0°
20°S
120°E
180°W
120°W
60°W
0
0.4
0.8
1.2
1.6
2
2.4
c Gradient change, 1.5°C RCP2.6 m 1869-1899
°C
0.4
0
-0.4
Ave.
1
2
3
4
5
6
7
8
9
10
11
12
13
Zonal gradient
Meridional gradient
d Gradient change, 2.0°C RCP4.5 m 1869-1899

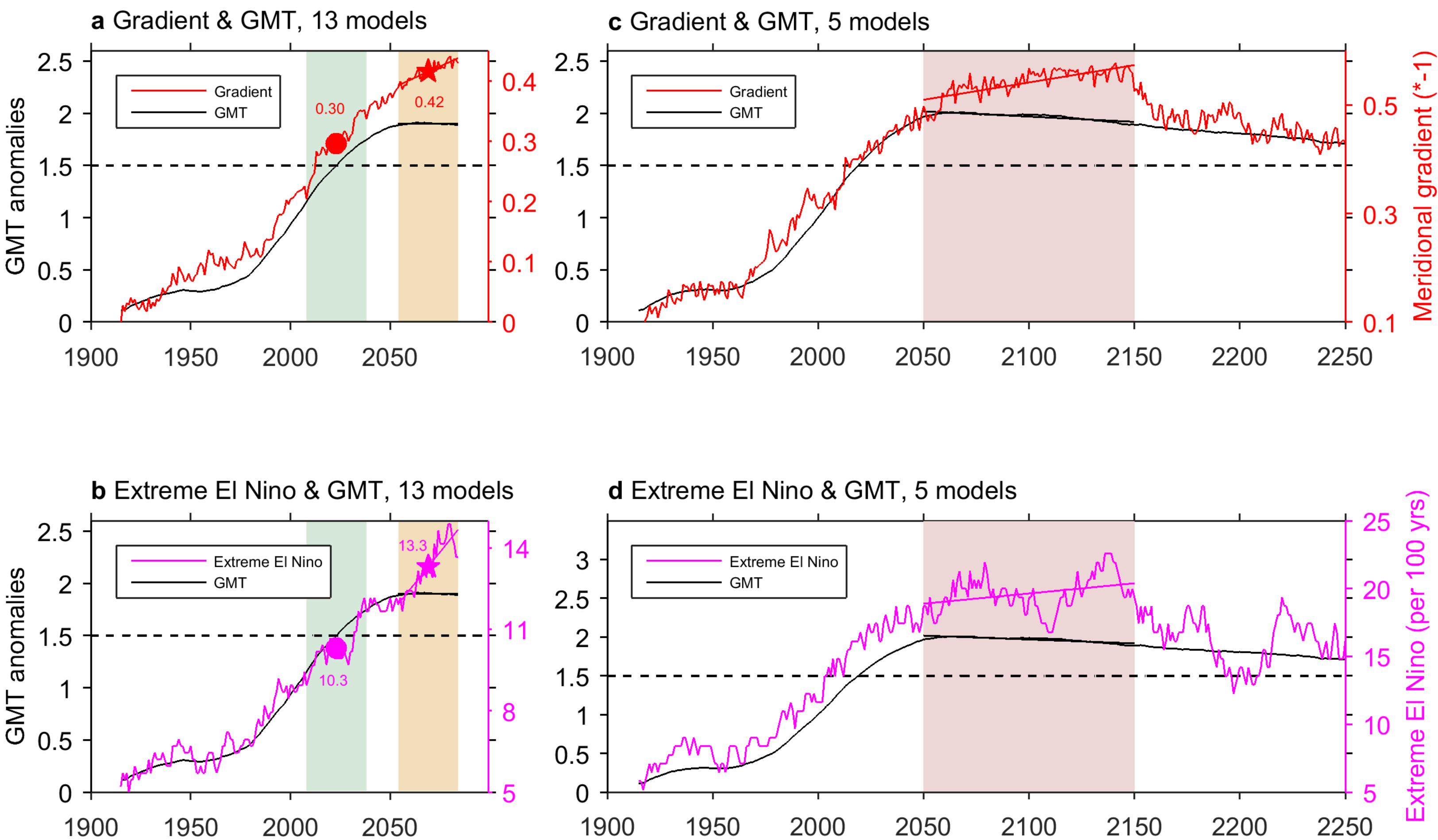

a Gradient & GMT, 13 models
c Gradient & GMT, 5 models
b Extreme El Nino & GMT, 13 models
d Extreme El Nino & GMT, 5 models
Gradient
GMT
Extreme El Nino
GMT anomalies
Meridional gradient (*-1)
Extreme El Nino (per 100 yrs)
0.30
0.42
10.3
13.3